

The effects of disorder and interactions on the Anderson transition in doped Graphene

Yun Song^a, Hongkang Song, and Shiping Feng

Department of Physics, Beijing Normal University, Beijing 100875, China

August 10, 2018

Abstract. We undertake an exact numerical study of the effects of disorder on the Anderson localization of electronic states in graphene. Analyzing the scaling behaviors of inverse participation ratio and geometrically averaged density of states, we find that Anderson metal-insulator transition can be introduced by the presence of quenched random disorder. In contrast with the conventional picture of localization, four mobility edges can be observed for the honeycomb lattice with specific disorder strength and impurity concentration. Considering the screening effects of interactions on disorder potentials, the experimental findings of the scale enlarges of puddles can be explained by reviewing the effects of both interactions and disorder.

1 Introduction

As a two-dimensional (2D) allotrope of carbon [1,2], graphene holds great promise for replacing conventional semiconductors on account of its unique electronic properties. In graphene, the σ -band formed by the sp^2 hybridized orbitals determines the robustness of the honeycomb structure, and the half-filled π -band provided with the Dirac-like electronic excitations is responsible for the unusual transport properties [3]. It has been observed in some experiments [4,5,6,7,8,9] that disorder has remarkable effects on the unusual electronic properties of graphene, and thus there has been a great deal of interest in recent years concerning the role of disorder in graphene.

Some experiments have confirmed the existence of metal-insulator transition (MIT) in disordered graphene [4,5,6], which suggests that the one-parameter scaling theory [10] may break down [11]. In accordance with the prediction of Klein paradox [12], the Dirac fermions are found to be robust against disorder in the 2D single valley Dirac model. In addition, the one-parameter scaling in single-valley Dirac Hamiltonian shows that [13,14], the logarithmic derivative $d\ln\sigma/d\ln L = \beta(\sigma)$ is a positive function and the scaling flow has no fixed point, indicating that the system always scales towards a metal. This scenario is different from what would be expected for the conventional 2D electron systems, where all states are localized for arbitrary weak disorder [10].

Recently, some numerical methods have been adopted in the study of the massless Dirac model with random potential [14,15,16,17,18] or the Anderson tight-binding model [19,20,21,22,23,24,25,26,27]. It is already clear that the single valley Dirac approximation is valid for graphene

with weak long-range impurities, but the intervalley scattering and chirality breaking scattering should be considered in the presence of strong short-range disorder. Therefore, the full tight-binding description of graphene with Anderson disorder becomes a popular alternative model. Some very recent simulations [22,23,24] have provided new evidence for the existence of MIT in graphene with short-range disorder by obtaining the mobility edges near the Fermi energy. However, a contrary view has been supported by the transfer-matrix approach [25] and kernel polynomial method [27] that all states in the Anderson tight-binding model are localized for arbitrary weak disorder. The possible reason for the disagreement to arise is that different measures and scaling rules are adopted in the above studies in an effort to distinguish localized states from delocalized ones.

In this paper, we introduce a new approach to scale the inverse participation ratio (IPR), which overcomes the unstable and unreliable problems caused by the primitive scaling of IPR with the negative first or second power of lattice size. We study the tight-binding Hamiltonian of the honeycomb lattice with randomly fluctuated disorder potentials, and an unique picture of Anderson MIT has been obtained. As expected, we find that all electronic states in graphene are localized by strong disorder. However, four mobility edges can be observed when we decrease the disorder strength until under a critical value W_c , and the electronic states within two nearest neighbor mobility edges are entirely extended or localized alternatively. Therefore, MIT can be introduced by changing the carrier density to move the Fermi surface across a certain mobility edge. Our results are in agreement with the very recent experimental suggestions, where a transition from localization to antilocalization has been achieved by decreasing the carrier density in graphene samples [6].

^a e-mail: yunsong@bnu.edu.cn

On the other hand, the sources of the coexistence of electron and hole puddles observed by the scannable single-electron transistor (SET) have been proved to be both the substrate-induced structural distortion as well as chemical doping. While the length scale of density fluctuations, which is more than 150nm [7], is extremely larger than the disorder length scale introduced by the short-range scatters. In this paper, we show that the unexpected large disorder length scale observed by SET can be explained by the screening effect of interactions on disorder, suggesting that the electron-electron interactions should be taken into account. Besides, the delocalization effect of interactions through screening disorder potentials can also introduce the zero-bias anomaly at Fermi surface [28,29,30].

In this paper we address the following issues related to the effect of disorder in graphene: (1) Whether there exists the mobility edge to separate the localized states from the delocalized states in disordered graphene? A distinctive scenario of Anderson MIT with four mobility edges have been observed in graphene with quenched random disorder; (2) How to measure the localization length of a localized electronic state by IPR? We present a new method to set the lattice size scaling of IPR, which can give the localization length of electronic state precisely; (3) What is the role of interactions in disordered graphene? The screening effect of the short-rang interactions on disorder potentials is found to have strong affection for the scale enlarges of puddles.

The paper is organized as follows: In section. 2.1 we present the fully tight-binding description of the disordered graphene. In section. 2.2 and 2.3, we discuss the lattice size scaling of the IPR and the geometrically averaged density of states (GADOS) respectively, and show the scaling method relevant for the subsequent discussions. Next we show our findings regarding the static disorder in graphene in section. 3. In addition, the screening effects of the electron-electron interactions on the disorder potentials are presented in section. 4. The principal findings of this paper are summarized in section. 5.

2 Theory

2.1 The Anderson Tight-binding Model

The Anderson tight-binding Hamiltonian [31,32] for the disordered graphene can be expressed as

$$H_{AM} = -t \sum_{\langle ij \rangle} c_i^\dagger c_j + \sum_i \epsilon_i c_i^\dagger c_i, \quad (1)$$

where c_i (c_i^\dagger) are annihilation (creation) operators of a fermion at site i , ϵ_i represent the on-site disorder energies, and t denote the hopping integrals between nearest neighbor (NN) sites, which are set to be unit in our calculations. We take the exact numerical approach to find all eigenenergies and eigenfunctions of the Hamiltonian given by Eq. (1) for a finite hexagonal lattice with the periodic boundary conditions. Besides, the numerical calculations

are performed with regard to the following three different disordered cases.

Firstly, in the presence of quenched random disorder, we introduce the box distributed Anderson disorder, and the on-site disorder energies ϵ_i in Eq. (1) are assumed to be independent random variables distributed between $-W/2$ and $W/2$. Therefore, the probability distribution of ϵ_i is given by

$$P(\epsilon) = W^{-1} \Theta(W/2 - |\epsilon|), \quad (2)$$

and the disorder strength is parameterized by the width W .

Secondly, to take into account the influences of the impurity potentials to the adjacent sites [21], the correlation length of disorder ζ is introduced and the on-site disorder energies ϵ_i in Eq. (1) can be replaced by the correlated disorder energy $\tilde{\epsilon}_i$ as

$$\tilde{\epsilon}_i = \sum_{l=1}^N \epsilon_l \exp(-|\mathbf{r}_i - \mathbf{r}_l|^2 / \zeta^2). \quad (3)$$

Where ϵ_l represent the "uncorrelated" disorder energies of the impurities at sites l , which have been defined in the first case.

Finally, in order to generalize this Hamiltonian by including electron-electron correlations, one must add an interaction term H_{int} onto the Anderson tight-binding model:

$$H = H_{AM} + H_{int}, \quad (4)$$

with

$$H_{int} = U \sum_i n_{i\uparrow} n_{i\downarrow} + \sum_{ij} V_{ij} n_i n_j. \quad (5)$$

Here $n_{i\sigma} = c_{i\sigma}^\dagger c_{i\sigma}$ is the local charge-density operator with $\sigma = \uparrow, \downarrow$, U represent the on-site interactions, and V_{ij} denote the non-local interactions between electrons at sites i and j . To compare with the experimental finding about the enlarges of puddles [7], here we consider a case of the binary alloy disorder, in which the probability distribution function of the on-site disorder energies is given by

$$p(\epsilon_i) = x\delta(\epsilon_i - W) + (1-x)\delta(\epsilon_i), \quad (6)$$

where x is the fraction of the lattice sites with energies $\epsilon_i = W$, and W represents the on-site energy splitting.

2.2 The Lattice Size Scaling of IPR

One of the widely used quantities to measure the Anderson localization of electronic states in disordered systems is called IPR, which is defined as [33,34]

$$I_2(E_n) = \sum_{i=1}^N |\Psi_n(r_i)|^4, \quad (7)$$

where E_n ($n=1, \dots, N$) and $\Psi_n(r_i)$ are the eigenenergies and eigenfunctions of a disordered finite lattice with N sites.

Since the eigenenergies of a finite lattice are always discrete, it is more convenient to introduce a continuous energy-dependent IPR as

$$I_2(\omega, N) = \frac{\sum_{i=1}^N \Theta(\frac{\gamma}{2} - |\omega - E_n|) I_2(E_n)}{\sum_{i=1}^N \Theta(\frac{\gamma}{2} - |\omega - E_n|)}, \quad (8)$$

where ω represents energy, and γ is a very small energy bin for the average. Since IPR of extended states are proportional to $1/L^d$ and go to zero in the infinite lattice limit $L \rightarrow \infty$, it is not difficult to identify extended states by doing lattice size scaling of IPR. Here d denotes the dimension of the system, and L represents the lattice size with $N = L^d$. However, the lattice size scaling of IPR for a localized state is found to be more complicated than expected [35,36,37,38].

The wave function of Anderson localized states decays exponentially as $|\psi(r)| \sim \exp(-|r - r_0|/\xi_{loc})$, where ξ_{loc} is the localization length. When the lattice size L is much larger than the localization length, IPR is a size-independent constant I_2^0 , and the localization length can be obtained easily by $\xi_{loc} = (I_2^0)^{-1/d}$ [38]. However, we can not always perform calculations satisfying the condition $L \gg \xi_{loc}$ on account of the limited capacity of the numerical calculations. When the lattice sizes are comparable to or even smaller than the localization length ξ_{loc} , L becomes a variable to the function of IPR. Later a simple lattice size scaling formula $1/L^\alpha$ has been suggested. Unfortunately, this IPR scaling can mistakenly regard a localized state as an extended state in some cases. For example, the exact scaling formula of IPR in one-dimensional (1D) systems with box distributed disorder has been obtained as [38]

$$I_2(\omega, L) = I_2(\omega, \infty) \coth(L/2\xi_{loc}(\omega)), \quad (9)$$

with $\xi_{loc}(\omega) = I_2^{-1}(\omega, \infty)$. It is obvious that the simple formula $1/L^\alpha$ is not a proper approximation in considerable large lattice size region to scale IPR. Certainly, there are also exceptions for the conditions with $L \gg \xi_{loc}$ and $L \ll \xi_{loc}$, where we can choose $\alpha = 0$ or $\alpha = 2$ respectively.

Unlike the 1D disordered system, the exact expression for IPR has not been obtained for the 2D finite systems. Therefore, we introduce a Taylor series to scale IPR by

$$I_2(\omega, L) = I_2(\omega, \infty) + \frac{a_1(\omega)}{L} + \frac{a_2(\omega)}{L^2} + \frac{a_3(\omega)}{L^3} + \dots, \quad (10)$$

where $a_n(\omega)$ is the n -th Taylor parameter. The minimum radius of convergence is found to be $R_{min} = 0.1$ in our studies, and to make all Taylor series adopted convergent, we have to do calculations when lattices meet the condition of $L > 1/R_{min} = 10$. For convenience, we employ a polynomial formula consist of the front five terms in Eq. (10) since the contributions of high-order terms are negligible. As shown in Fig. 1, the new fitting is reasonable and practical since the intercept of an extended state is found to be zero or even a very small negative number, whereas the fitting curve of a localized state has a positive intercept in the infinite-lattice limit. We have

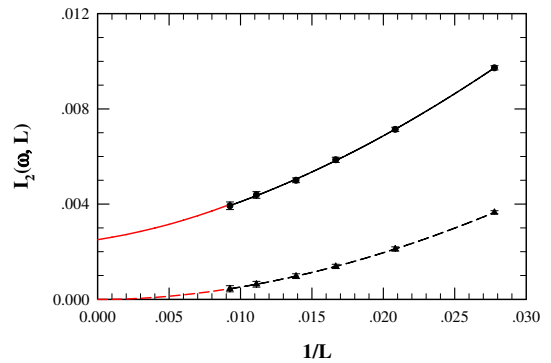


Fig. 1. (color online) The lattice size scaling of IPR $I_2(\omega, L)$ for a localized (circles) and an extended (triangles) state. The black lines are the fitting curves obtained by the polynomial formula shown in Eq. (10), and the red lines show the extensions of the fitting curves to the infinite lattice limit $L \rightarrow \infty$.

checked the above fitting method by the disordered cubic lattice [39], and good agreements have been achieved with the accepted scaling theories [10]. Especially, we find that the fitting curves of extended states can be approximated by $I_2(\omega, L) \propto 1/L^2$, in accordance with the prediction of some other theories. On the other hand, when the electronic state is localized, the five parameters are all found to have non-zero values, but the low-order terms play the main roles. As shown by the solid line in Fig. 1, there exists a finite intercept $I_2(\omega, \infty)$ for a localized state, and its localization length can be obtained by

$$\xi_{loc}(\omega) = \frac{1}{\sqrt{I_2(\omega, \infty)}}. \quad (11)$$

To sum up, the new scaling method of IPR has the advantage in distinguishing explicitly the localized states with extended states, and in addition we can acquire the localization length precisely by the intercept obtained in the infinite-size limit.

2.3 Measure Anderson Localization by GADOS

It has been proposed that Anderson localization can be measured by an order parameter $\rho_g(\omega)$, called GADOS, which is obtained by geometrically averaging the local DOS (LDOS) of each site as

$$\rho_g(\omega) = \frac{1}{N_s} \sum_{m=1}^{N_s} \left[\prod_i^N \rho(r_i, \omega) \right]^{1/N}, \quad (12)$$

with

$$\rho(r_i, \omega) = \frac{\sum_{n=1}^N \Theta(\frac{\gamma}{2} - |\omega - E_n|) \rho(r_i, E_n)}{\sum_{i=1}^N \Theta(\frac{\gamma}{2} - |\omega - E_n|)}. \quad (13)$$

Where $\rho(r_i, E_n) = |\Psi_n(r_i)|^2$ is the LDOS at site i for the n -th eigenstate Ψ_n , N_s represents the number of disorder

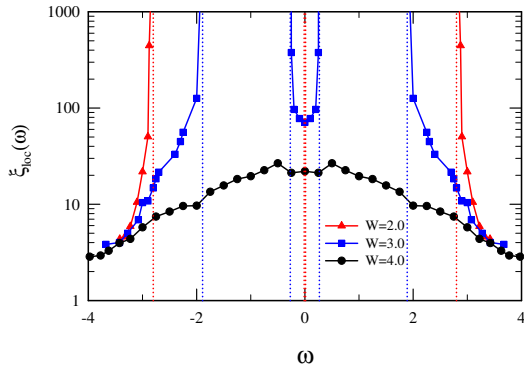


Fig. 2. (color online) The energy dependencies of the localization length $\xi_{loc}(\omega)$ of graphene with Anderson disorder. The box distribution is adopted for the on-site energies of every sites with disorder strength $W=2.0$ (red triangles), 3.0 (blue squares), and 4.0 (black circles). The dotted lines denote the mobility edges.

configurations to be averaged, and the energy bin γ plays the same role as in Sec. 2.2.

For the infinite-dimensional disordered system, it has been defined that Anderson transition happens when $\rho_g(\epsilon_F)$ vanishes completely at Fermi surface ϵ_F . This criterion has been introduced to investigate the competition between Anderson transition and Mott MIT in the infinite-dimensional systems within the dynamical mean-field theory [40,41]. While, in the numerical calculation for a finite lattice of low-dimensional disordered system, a finite energy bin γ has to be introduced. As a result, GADOS is a function of lattice size, and its lattice size scaling should be introduced to detect the Anderson MIT.

In Ref. [38], we have examined the lattice size scale of GADOS and found that, for any nonzero energy bin γ , ρ_g decays exponentially with the increasing of lattice size for a localized electronic state. On the contrary, there is no significant variation of ρ_g with the increasing of lattice size for a delocalized state. Therefore, it is not difficult to distinguish localized states from extended states by the lattice size scaling of GADOS. In this paper, we use GADOS scaling to check our results obtained by IPR scaling about whether the electronic states are localized or not, and good agreements have been achieved.

3 Localization in disordered graphene

The scaling theories of localization have proved that all electronic states should be localized in the conventional 2D systems with arbitrary weak disorder [10]. Comparing with the parabolic DOS of conventional 2D system, graphene has a special band structure with zero weight at Dirac points. Applying the Dirac model with random potentials to the weakly disordered graphene, some studies have confirmed the existence of the antilocalized electronic states [15,14] because of the insensitivity of the Dirac fermions to the disordered external electrostatic potentials. On the other hand, strong disorder can manifestly enhance the DOS at Dirac points and strongly affect

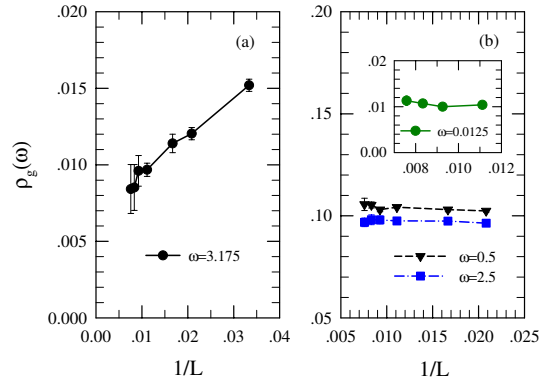


Fig. 3. (color online) The lattice size scaling of GADOS of electronic states with different energies: (a) $\omega = 3.175$ (black circles), and (b) $\omega = 0.5$ (black triangles) and 2.5 (blue squares). Inset: the scaling of GADOS close to the Dirac point with $\omega = 0.0125$ (green circles). The disorder strength of Anderson disorder is $W=2.0$.

the electronic properties. For this reason, our study will concentrate firstly on the evolutions of electronic states in the whole energy band with the increasing of disorder strength.

We study the Anderson tight-binding model on a hexagonal lattice by exact numerical simulations, where the largest lattices could be 120×120 . Applying the IPR scaling method introduced in Sec. 2.2, the localization lengths of localized electronic states are obtained for different disorder strength W . As shown in Fig. 2, it is obvious that disordered graphene has a quite different scenario of Anderson localization than the conventional 2D systems with disorder. When disordered strength $W = 2$ or 3 , we find energy regions consist of the localized electronic states separated by the mobility edges from the regions of extended ones, where the physical observable is the finite localization lengths of localized states. Close to the top and bottom of the whole energy band, we obtain two symmetrical mobility edges at $\omega = \pm\omega_{c1}$. In addition, two mobility edges appear near the Fermi surface ($\epsilon_F = 0$) with $\omega = \pm\omega_{c2}$ ($\omega_{c2} < \omega_{c1}$), suggesting the electronic states around the Fermi surface are also easier to be localized by the scattering with the disorder potentials. Furthermore, all electronic states can be localized when the disorder strength is increased larger than $W'_c = 3.10$.

The region close to the Dirac points is very important, and people show great interests in the possible existence of the antilocalized electronic states at there. However, the scaling results are affected magnificently by the relative big errors for IPR since the DOS is quite low in the vicinity of Dirac points. In addition, it is well known that to distinguish an extended state from a weakly localized state with large localization length is very difficult. To make our finding more convincing, we also use the scaling of GADOS to measure Anderson localization in disordered graphene. We find very good agreements between the scalings of GADOS and IPR.

In Fig. 3, we show the lattice size dependencies of GADOS for some representative energies when $W = 2$. In

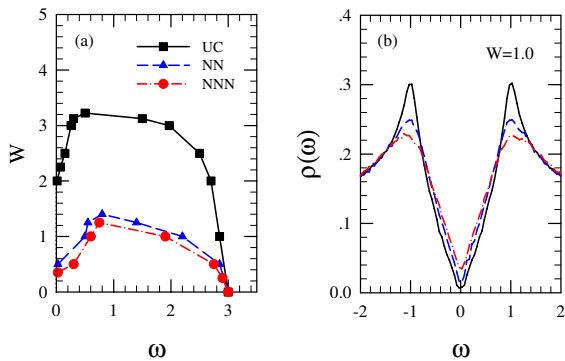


Fig. 4. (color online) (a) The energy dependencies of the critical disorder strength $W_c(\omega)$ of graphene with correlated disorder; (b) The effects of the correlations of disorder on DOS around Fermi surface $\omega = 0$. The solid (black), dashed (blue), and dashed-dotted (red) lines represent respectively the results of point defects, NN scatters and both NN and NNN scatters.

Fig. 3(a), GADOS of $\omega = 3.25$ increases manifestly with the increasing of $1/L$, suggesting the state is localized. On the contrary, GADOS of the other two extended states with energy $\omega = 0.5$ and 2.5 are both lattice size independent as shown in Fig. 3(b). When $\omega = 0.0125$, we have performed the scaling of GADOS very carefully and precisely by averaging more than two hundreds of disorder configurations for lattice with $L = 120$. As shown by the insert in Fig. 3(b), the lattice size independent behavior of GADOS indicates clearly that the electronic states quite close to the Dirac points are still extended, in accordance with the result obtained by the IPR scaling. Our result suggests that the prediction of single valley model, i.e. Dirac Fermions can not be localized by disorder, is reasonable in weakly disordered graphene since no intervalley scattering can be stimulated by very weak disorder. In addition, it is obvious that the Anderson MIT can be introduced by only changing the carrier density to move the Fermi surface from extended region to localized region with fixed disorder strength. Recently, a transition between localization and antilocalization has been observed experimentally in graphene when the carrier density is decreased [6]. Therefore, our result about Anderson localization with four mobility edges help clarify this experimental observation of MIT in graphene. In addition, our findings suggest that the delocalization is closely related to the linear dispersion near the Dirac points which may suppress the inter-valley scattering. And further investigations are to be done in the future study.

The electrostatic coulomb potentials of the surface absorptions or the adatoms in the substrate for graphene should be described by Eq. (3), in which the correlations between the disorder potentials of individual sites are considered. Owing to the screening effect of electrons, the long-range correlations of disorder could be neglected. Here we name the uncorrelated and short-range correlated disorder as point defects and short-range scatters respectively. In Fig. 4, we show the effects of the nearest-neighbor (NN) and next NN (NNN) scatters on the localization of

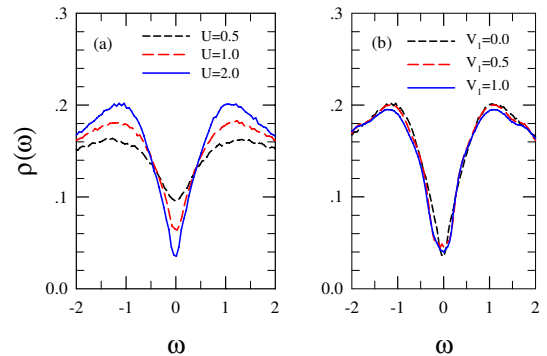


Fig. 5. (color online) The evolutions of DOS of graphene with disorder strength $W = 4$ and short-range interactions: (a) there are only on-site interactions $U = 0.5$ (black dashed line), 1.0 (red dashed line), and 2.0 (blue solid line), and (b) the on-site interactions are fixed as $U = 2.0$, and the NN interactions are given as $V_1 = 0.0$ (black dashed line), 0.5 (red dashed line), and 1.0 (blue solid line).

electronic states. The correlation length ζ is set as $1.5a$, which is the same as the parameters chosen in Ref. [42], and the blue dashed and red dash-dotted lines reveal the energy dependence of the critical disorder strength $W_c(\omega)$ for graphene with the NN scatters only and both NN and NNN scatters, respectively. For the convenience of comparison, we also show the results of uncorrelated point defects (black solid line). It is obvious that the picture of Anderson MIT for short-range scatters is the same as that of the point defects. While, the short-range correlations of disorder have strong effects to localize the electronic states. As to why the critical strengths of disorder W_c for localizing the states are greater for uncorrelated disorder than the correlated ones, the effective disorder strength is actually enhanced a lot as we add the influences of the impurity potentials of the adjacent sites onto the uncorrelated on-site energy of a certain site directly. As a result, the localization of electronic states is enhanced accordingly when the re-scaling is not introduced to reduce the original disorder strength.

4 The interactions and electron-hole puddles in disordered graphene

In pure graphene, the influence of short-range interactions on electronic properties has been investigated by the dynamical mean-field theory (DMFT) [43]. The Dirac sea state is found to remain stable against local many-body interactions since the interactions in graphene are much smaller than the Mott critical value $U_c = 13.3t$ [43]. In the present of disorder, the combine effects of interactions and disorder will have strong influences on the LDOS and also the localization of electronic states. It has been proved recently by the statistic DMFT calculations [38] that the Hartree-Fock approximation (HFA) could give reasonable results for the conventional 2D Anderson-Hubbard model

when the interactions U are smaller than the energy bandwidth D . Based on the predictions for the many-body effect in graphene given by Ref. [3], we study the Anderson-Hubbard mode with weak interactions in the region of $U = 0.5t$ to $4.0t$ within HFA.

In conventional 2D disordered systems, the zero-bias anomaly at Fermi surface [28,29,30] arises from the interplay between disorder and interactions, which indicates the delocalization effects of interactions on localized electronic states [44]. In the same manner, we observe the DOS of disordered graphene at Fermi surface to show the delocalization effects of the short-range interactions. Firstly, we only consider the effects of the on-site interactions U , and as shown in Fig. 5(a), significant decreasing of the DOS around the Fermi surface appears when we increase U from 0.5 to 4.0. On the contrary, the long-rang interactions are found to have less effect to the zero-bias anomaly at Fermi surface. In Fig. 5(b), we plot the DOS for graphene with different NN interactions and fixed U , and it is obvious that even the effects of NN interactions are still weak and negligible. Therefore, we predict that the on-site interaction is the key point in the study of the screening effects of interactions in disordered graphene. The local effect of interactions can be understood by calculating the screened potential $v_i = \epsilon_i(1 - U\chi_{ii})$, where the local charge susceptibility is defined as $\chi_{ii} = -\partial n_i / \partial \epsilon_i$. It is obvious that the screening effect in localized phase is expected to be less than in metallic phase since χ_{ii} is restrained for site with small LDOS at Fermi level. We find in the paramagnetic phase that the on-site interactions have strong effects to delocalize the electronic states by increasing the localization lengths accordingly.

Since The LDOS at Fermi surface ϵ_F is detectable, to compare with the experimental results, we calculate the evolution of $\rho(r_i, \epsilon_F)$ with the on-site interactions U for a particular binary disordered configuration. As shown in Fig. 6 and Fig. 7, the length scale of density variations of LDOS for $U = 0.0$ is much smaller than that for $U = 2.0$ and 4.0 . Compared with the quarter-filling case, the delocalization effects of interactions are not remarkable when the system is half-filled. It is obvious that the states at Dirac points are strongly localized at half-filling with $W = 4$. This further proves the results we obtained in the previous section from a different perspective. The regions of electron-rich and hole-rich puddles have been observed by the experiment of using scanning single-electron transistor to map the LDOS of graphene sheet [7]. The smallest length scale on which density variations is observed roughly 150nm, which is apparently significantly larger than the intrinsic disorder length scale as approximately 30nm in the graphene samples. There arises the question of why there exists such a big difference between the length scales of the LDOS and intrinsic impurities. Our results predict that the interactions play an important role in the electron-hole puddles observed by experiment, where the screening effects of the on-site interactions on disorder potentials can enlarge the length scale of LDOS significantly.

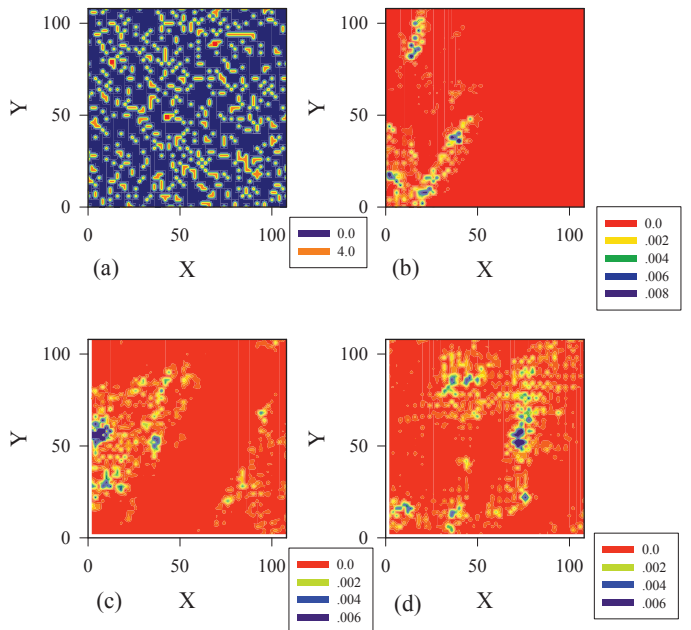


Fig. 6. (color online) (a) The disorder configuration of an 108×108 lattice with binary disorder. The on-site energy splitting is $W = 4$; The corresponding LDOS of an eigenstate right at the Fermi level for different on-site interactions: (b) $U = 0.0$, (c) 2, and (d) 4.0. The systems are all half-filled with impurity concentration $x = 0.2$.

5 Conclusions

We have studied numerically the Anderson tight-binding model of the finite hexagonal lattices and found that, unlike the conventional 2D disordered systems, there is a unique picture of the Anderson localization with four mobility edges in disordered graphene. We predict that Anderson MIT can be achieved in graphene by changing the carrier density to make a move of the Fermi surface across the mobility edges. In addition, we have found that the length scale of LDOS is considerably enhanced by the on-site interactions when the screening effects of interactions on the disorder potentials are also taken into consideration.

Besides, the measure of Anderson localization by IPR has also been discussed, and a polynomial formula has been introduced for the lattice size scaling of IPR. As a result, precise localization length of the localized electronic state can be obtained by the intercept found in the infinite-size limit.

Acknowledgments

We are grateful to W. A. Atkinson for reading the manuscript and valuable comments. The work was supported by the project-sponsored by SRF for ROCS, SEM, the NSFC of China, under Grant Nos. 10974018 and 10774015, and the National Basic Research Program of China (Grant Nos. 2011CBA00108 and 2007CB925004).

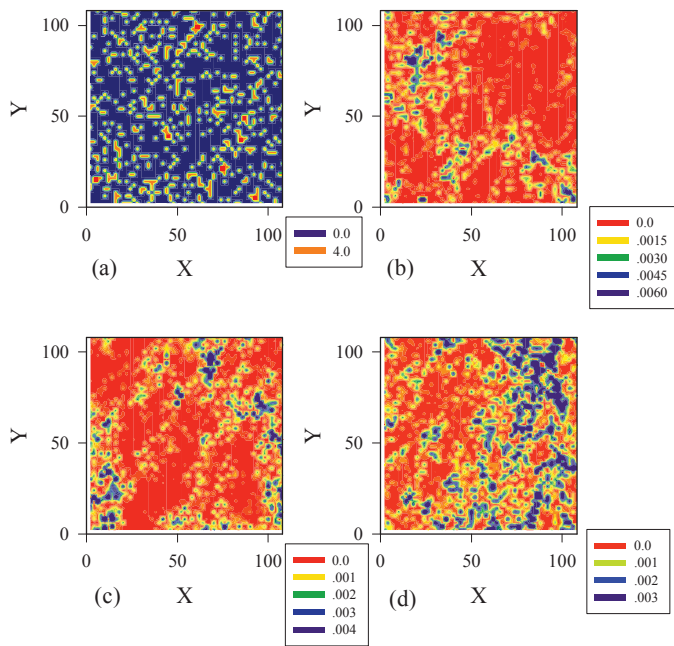


Fig. 7. (color online) The disorder configuration and the corresponding LDOS are shown for the same parameters as in Fig. 6, except that the systems are all quarter-filled.

References

References

1. Novoselov K S, Geim A K, Morozov S V, Jiang D, Zhang Y, Dubonos S V, Grigorieva I V and Firsov A A 2004 *Science* **306** 666; Novoselov K S, Geim A K, Morozov S V, Jiang D, Katsnelson M I, Grigorieva I V, Dubonos S V and Firsov A A 2005 *Nature* **438** 197
2. Zhang Y, Tan Y-W, Stormer H L and Kim P 2005 *Nature* **438** 201
3. Castro Neto A H, Guinea F, Peres N M R, Novoselov K S and Geim A K 2009 *Rev. Mod. Phys.* **81** 109
4. Bostwick A, McChesney J L, Emtsev K V, Seyller T, Horn K, Kevan S D and Rotenberg E 2009 *Phys. Rev. Lett.* **103** 056404
5. Adam S, Cho S, Fuhrer M S and Das Sarma S 2008 *Phys. Rev. Lett.* **101** 046404
6. Tikhonenko F V, Kozikov A A, Savchenko A K and Gorbachev R V 2009 *Phys. Rev. Lett.* **103** 226801
7. Martin J, Akerman N, Ulbricht G, Lohmann T, Smet J H, Von Klitzing K and Yacoby A 2008 *Nature Phys.* **4** 144
8. Chen J-H, Jang C, Adam S, Fuhrer M S, Williams E D and Ishigami M 2008 *Nature Phys.* **4** 377
9. Tan Y-W, Zhang Y, Bolotin K, Zhao Y, Adam S, Hwang E H, Das Sarma S, Stormer H L and Kim P 2007 *Phys. Rev. Lett.* **99** 246803
10. Lee P A and Ramakrishnan T V 1985 *Rev. Mod. Phys.* **57** 287
11. Krapivsky P L and Luck J M, 2011 *J. Stat. Mech.* P02031.
12. Katsnelson M I, Novoselov K S and Geim A K 2006 *Nature Phys.* **2** 620; Calogeracos A and Dombey N 1999 *Contemp. Phys.* **40** 313; Klein O 1929 *Z. Phys.* **53** 157
13. Bardarson J H, Tworzydło J, Brouwer P W and Beenakker C W J 2007 *Phys. Rev. Lett.* **99** 106801

14. Nomura K, Koshino M and Ryu S, 2007 *Phys. Rev. Lett.* **99** 146806
15. Nomura K and MacDonald A H 2007 *Phys. Rev. Lett.* **98** 076602
16. Ziegler K, Dora B and Thalmeier P 2009 *Phys. Rev. B* **79** 235431; Ziegler K 2008 *Phys. Rev. Lett.* **100** 166801; 2008 *Phys. Rev. B* **78** 125401
17. Guinea F, Horowitz B and Le Doussal P 2008 *Phys. Rev. B* **77** 205421
18. Foster M S and Aleiner I L 2008 *Phys. Rev. B* **77** 195413
19. Pereira V M, Lopes dos Santos J M B and Castro Neto A H 2008 *Phys. Rev. B* **77** 115109
20. Wu S, Jing L, Li Q, Shi Q W, Chen J, Su H, Wang X and Yang J 2008 *Phys. Rev. B* **77** 195411
21. Zhang Y-Y, Hu J, Bernevig B A, Wang X R, Xie X C and Liu W M 2009 *Phys. Rev. Lett.* **102** 106401
22. Wu S and liu F 2010 arXiv: 1001.2057
23. Amini M, Jafari S A and Shahbazi F 2009 *Eur. Phys. Lett.* **87** 37002
24. Naumis G G 2007 *Phys. Rev. B* **76** 153403
25. Xiong S-J and Xiong Y 2007 *Phys. Rev. B* **76** 214204
26. Pershoguba S S, Skrypnyk Y V and Loktev V M 2009 *Phys. Rev. B* **80** 214201
27. Schubert G, Schleede J and Fehske H 2009 *Phys. Rev. B* **79** 235116
28. Efros A L and Shklovskii B I 1975 *J. Phys. C: Solid State Phys.* **8** L49
29. Efros A L 1976 *J. Phys. C: Solid State Phys.* **9** 2021
30. Altshuler B L and Aronov A G 1985 *Electron-Electron Interactions in Disordered Systems* Vol. **10** of *Modern Problems in Condensed Matter Sciences* (North-Holland)
31. Anderson P W 1958 *Phys. Rev.* **109** 1492
32. Evers F and Mirlin A D 2008 *Rev. Mod. Phys.* **80** 1355
33. Thouless D J 1974 *Phys. Rep.* **13** 93
34. Wegner F J 1980 *Z. Phys. B* **36** 209
35. Brndiar J and Markos P 2006 *Phys. Rev. B* **74** 153103
36. Cuevas E 2002 *Phys. Rev. B* **66** 233103
37. Zekri L, Bouamrane R, Zekri N and Brouers F 2000 *J. Phys. Condens. Matter* **12** 283
38. Song Y, Atkinson W A and Wortis R 2007 *Phys. Rev. B* **76** 045105
39. Sun J, He Long, Yang C and Song Y 2011 unpublished
40. Dobrosavljevic V and Kotliar G 1997 *Phys. Rev. Lett.* **78** 3943
41. Byczuk K, Hofstetter W and Vollhardt D 2005 *Phys. Rev. Lett.* **94** 056404
42. Wakabayashi K, Takane Y and Sigrist M 2007 *Phys. Rev. Lett.* **99** 036601
43. Jafari S A 2009 *Eur. Phys. J. B* **68** 537
44. Song Y, Bulut S, Wortis R and Atkinson W A 2009 *J. Phys. Condens. Matter* **21** 385601